Fermilab-Pub-12/319-E

Measurement of Leptonic Asymmetries and Top Quark Polarization in $t\bar{t}$ Production

V.M. Abazov,[32] B. Abbott,[69] B.S. Acharya,[26] M. Adams,[46] T. Adams,[44] G.D. Alexeev,[32] G. Alkhazov,[36] A. Alton[a],[58] G. Alverson,[57] A. Askew,[44] S. Atkins,[55] K. Augsten,[7] C. Avila,[5] F. Badaud,[10] L. Bagby,[45] B. Baldin,[45] D.V. Bandurin,[44] S. Banerjee,[26] E. Barberis,[57] P. Baringer,[53] J.F. Bartlett,[45] U. Bassler,[15] V. Bazterra,[46] A. Bean,[53] M. Begalli,[2] L. Bellantoni,[45] S.B. Beri,[24] G. Bernardi,[14] R. Bernhard,[19] I. Bertram,[39] M. Besançon,[15] R. Beuselinck,[40] P.C. Bhat,[45] S. Bhatia,[60] V. Bhatnagar,[24] G. Blazey,[47] S. Blessing,[44] K. Bloom,[61] A. Boehnlein,[45] D. Boline,[66] E.E. Boos,[34] G. Borissov,[39] T. Bose,[56] A. Brandt,[72] O. Brandt,[20] R. Brock,[59] A. Bross,[45] D. Brown,[14] J. Brown,[14] X.B. Bu,[45] M. Buehler,[45] V. Buescher,[21] V. Bunichev,[34] S. Burdin[b],[39] C.P. Buszello,[38] E. Camacho-Pérez,[29] B.C.K. Casey,[45] H. Castilla-Valdez,[29] S. Caughron,[59] S. Chakrabarti,[66] D. Chakraborty,[47] K.M. Chan,[51] A. Chandra,[74] E. Chapon,[15] G. Chen,[53] S. Chevalier-Théry,[15] D.K. Cho,[71] S.W. Cho,[28] S. Choi,[28] B. Choudhary,[25] S. Cihangir,[45] D. Claes,[61] J. Clutter,[53] M. Cooke,[45] W.E. Cooper,[45] M. Corcoran,[74] F. Couderc,[15] M.-C. Cousinou,[12] A. Croc,[15] D. Cutts,[71] A. Das,[42] G. Davies,[40] S.J. de Jong,[30,31] E. De La Cruz-Burelo,[29] F. Déliot,[15] R. Demina,[65] D. Denisov,[45] S.P. Denisov,[35] S. Desai,[45] C. Deterre,[15] K. DeVaughan,[61] H.T. Diehl,[45] M. Diesburg,[45] P.F. Ding,[41] A. Dominguez,[61] A. Dubey,[25] L.V. Dudko,[34] D. Duggan,[62] A. Duperrin,[12] S. Dutt,[24] A. Dyshkant,[47] M. Eads,[61] D. Edmunds,[59] J. Ellison,[43] V.D. Elvira,[45] Y. Enari,[14] H. Evans,[49] A. Evdokimov,[67] V.N. Evdokimov,[35] G. Facini,[57] L. Feng,[47] T. Ferbel,[65] F. Fiedler,[21] F. Filthaut,[30,31] W. Fisher,[59] H.E. Fisk,[45] M. Fortner,[47] H. Fox,[39] S. Fuess,[45] A. Garcia-Bellido,[65] J.A. García-González,[29] G.A. García-Guerra[c],[29] V. Gavrilov,[33] P. Gay,[10] W. Geng,[12,59] D. Gerbaudo,[63] C.E. Gerber,[46] Y. Gershtein,[62] G. Ginther,[45,65] G. Golovanov,[32] A. Goussiou,[76] P.D. Grannis,[66] S. Greder,[16] H. Greenlee,[45] G. Grenier,[17] Ph. Gris,[10] J.-F. Grivaz,[13] A. Grohsjean[d],[15] S. Grünendahl,[45] M.W. Grünewald,[27] T. Guillemin,[13] G. Gutierrez,[45] P. Gutierrez,[69] S. Hagopian,[44] J. Haley,[57] L. Han,[4] K. Harder,[41] A. Harel,[65] J.M. Hauptman,[52] J. Hays,[40] T. Head,[41] T. Hebbeker,[18] D. Hedin,[47] H. Hegab,[70] A.P. Heinson,[43] U. Heintz,[71] C. Hensel,[20] I. Heredia-De La Cruz,[29] K. Herner,[58] G. Hesketh[f],[41] M.D. Hildreth,[51] R. Hirosky,[75] T. Hoang,[44] J.D. Hobbs,[66] B. Hoeneisen,[9] J. Hogan,[74] M. Hohlfeld,[21] I. Howley,[72] Z. Hubacek,[7,15] V. Hynek,[7] I. Iashvili,[64] Y. Ilchenko,[73] R. Illingworth,[45] A.S. Ito,[45] S. Jabeen,[71] M. Jaffré,[13] A. Jayasinghe,[69] M.S. Jeong,[28] R. Jesik,[40] K. Johns,[42] E. Johnson,[59] M. Johnson,[45] A. Jonckheere,[45] P. Jonsson,[40] J. Joshi,[43] A.W. Jung,[45] A. Juste,[37] K. Kaadze,[54] E. Kajfasz,[12] D. Karmanov,[34] P.A. Kasper,[45] I. Katsanos,[61] R. Kehoe,[73] S. Kermiche,[12] N. Khalatyan,[45] A. Khanov,[70] A. Kharchilava,[64] Y.N. Kharzheev,[32] I. Kiselevich,[33] J.M. Kohli,[24] A.V. Kozelov,[35] J. Kraus,[60] S. Kulikov,[35] A. Kumar,[64] A. Kupco,[8] T. Kurča,[17] V.A. Kuzmin,[34] S. Lammers,[49] G. Landsberg,[71] P. Lebrun,[17] H.S. Lee,[28] S.W. Lee,[52] W.M. Lee,[45] X. Lei,[42] J. Lellouch,[14] H. Li,[11] L. Li,[43] Q.Z. Li,[45] J.K. Lim,[28] D. Lincoln,[45] J. Linnemann,[59] V.V. Lipaev,[35] R. Lipton,[45] H. Liu,[73] Y. Liu,[4] A. Lobodenko,[36] M. Lokajicek,[8] R. Lopes de Sa,[66] H.J. Lubatti,[76] R. Luna-Garcia[g],[29] A.L. Lyon,[45] A.K.A. Maciel,[1] R. Madar,[15] R. Magaña-Villalba,[29] S. Malik,[61] V.L. Malyshev,[32] Y. Maravin,[54] J. Martínez-Ortega,[29] R. McCarthy,[66] C.L. McGivern,[41] M.M. Meijer,[30,31] A. Melnitchouk,[60] D. Menezes,[47] P.G. Mercadante,[3] M. Merkin,[34] A. Meyer,[18] J. Meyer,[20] F. Miconi,[16] N.K. Mondal,[26] M. Mulhearn,[75] E. Nagy,[12] M. Naimuddin,[25] M. Narain,[71] R. Nayyar,[42] H.A. Neal,[58] J.P. Negret,[5] P. Neustroev,[36] T. Nunnemann,[22] D. Orbaker,[65] J. Orduna,[74] N. Osman,[12] J. Osta,[51] M. Padilla,[43] A. Pal,[72] N. Parashar,[50] V. Parihar,[71] S.K. Park,[28] R. Partridge[e],[71] N. Parua,[49] A. Patwa,[67] B. Penning,[45] M. Perfilov,[34] Y. Peters,[41] K. Petridis,[41] G. Petrillo,[65] P. Pétroff,[13] M.-A. Pleier,[67] P.L.M. Podesta-Lerma[h],[29] V.M. Podstavkov,[45] A.V. Popov,[35] M. Prewitt,[74] D. Price,[49] N. Prokopenko,[35] J. Qian,[58] A. Quadt,[20] B. Quinn,[60] M.S. Rangel,[1] K. Ranjan,[25] P.N. Ratoff,[39] I. Razumov,[35] P. Renkel,[73] I. Ripp-Baudot,[16] F. Rizatdinova,[70] M. Rominsky,[45] A. Ross,[39] C. Royon,[15] P. Rubinov,[45] R. Ruchti,[51] G. Sajot,[11] P. Salcido,[47] A. Sánchez-Hernández,[29] M.P. Sanders,[22] A.S. Santos[i],[1] G. Savage,[45] L. Sawyer,[55] T. Scanlon,[40] R.D. Schamberger,[66] Y. Scheglov,[36] H. Schellman,[48] S. Schlobohm,[76] C. Schwanenberger,[41] R. Schwienhorst,[59] J. Sekaric,[53] H. Severini,[69] E. Shabalina,[20] V. Shary,[15] S. Shaw,[59] A.A. Shchukin,[35] R.K. Shivpuri,[25] V. Simak,[7] P. Skubic,[69] P. Slattery,[65] D. Smirnov,[51] K.J. Smith,[64] G.R. Snow,[61] J. Snow,[68] S. Snyder,[67] S. Söldner-Rembold,[41] L. Sonnenschein,[18] K. Soustruznik,[6] J. Stark,[11]

D.A. Stoyanova,[35] M. Strauss,[69] L. Suter,[41] P. Svoisky,[69] M. Takahashi,[41] M. Titov,[15] V.V. Tokmenin,[32] Y.-T. Tsai,[65] K. Tschann-Grimm,[66] D. Tsybychev,[66] B. Tuchming,[15] C. Tully,[63] L. Uvarov,[36] S. Uvarov,[36] S. Uzunyan,[47] R. Van Kooten,[49] W.M. van Leeuwen,[30] N. Varelas,[46] E.W. Varnes,[42] I.A. Vasilyev,[35] P. Verdier,[17] A.Y. Verkheev,[32] L.S. Vertogradov,[32] M. Verzocchi,[45] M. Vesterinen,[41] D. Vilanova,[15] P. Vokac,[7] H.D. Wahl,[44] M.H.L.S. Wang,[45] J. Warchol,[51] G. Watts,[76] M. Wayne,[51] J. Weichert,[21] L. Welty-Rieger,[48] A. White,[72] D. Wicke,[23] M.R.J. Williams,[39] G.W. Wilson,[53] M. Wobisch,[55] D.R. Wood,[57] T.R. Wyatt,[41] Y. Xie,[45] R. Yamada,[45] S. Yang,[4] W.-C. Yang,[41] T. Yasuda,[45] Y.A. Yatsunenko,[32] W. Ye,[66] Z. Ye,[45] H. Yin,[45] K. Yip,[67] S.W. Youn,[45] J.M. Yu,[58] J. Zennamo,[64] T. Zhao,[76] T.G. Zhao,[41] B. Zhou,[58] J. Zhu,[58] M. Zielinski,[65] D. Zieminska,[49] and L. Zivkovic[71]

(The D0 Collaboration*)

[1]*LAFEX, Centro Brasileiro de Pesquisas Físicas, Rio de Janeiro, Brazil*
[2]*Universidade do Estado do Rio de Janeiro, Rio de Janeiro, Brazil*
[3]*Universidade Federal do ABC, Santo André, Brazil*
[4]*University of Science and Technology of China, Hefei, People's Republic of China*
[5]*Universidad de los Andes, Bogotá, Colombia*
[6]*Charles University, Faculty of Mathematics and Physics, Center for Particle Physics, Prague, Czech Republic*
[7]*Czech Technical University in Prague, Prague, Czech Republic*
[8]*Center for Particle Physics, Institute of Physics, Academy of Sciences of the Czech Republic, Prague, Czech Republic*
[9]*Universidad San Francisco de Quito, Quito, Ecuador*
[10]*LPC, Université Blaise Pascal, CNRS/IN2P3, Clermont, France*
[11]*LPSC, Université Joseph Fourier Grenoble 1, CNRS/IN2P3, Institut National Polytechnique de Grenoble, Grenoble, France*
[12]*CPPM, Aix-Marseille Université, CNRS/IN2P3, Marseille, France*
[13]*LAL, Université Paris-Sud, CNRS/IN2P3, Orsay, France*
[14]*LPNHE, Universités Paris VI and VII, CNRS/IN2P3, Paris, France*
[15]*CEA, Irfu, SPP, Saclay, France*
[16]*IPHC, Université de Strasbourg, CNRS/IN2P3, Strasbourg, France*
[17]*IPNL, Université Lyon 1, CNRS/IN2P3, Villeurbanne, France and Université de Lyon, Lyon, France*
[18]*III. Physikalisches Institut A, RWTH Aachen University, Aachen, Germany*
[19]*Physikalisches Institut, Universität Freiburg, Freiburg, Germany*
[20]*II. Physikalisches Institut, Georg-August-Universität Göttingen, Göttingen, Germany*
[21]*Institut für Physik, Universität Mainz, Mainz, Germany*
[22]*Ludwig-Maximilians-Universität München, München, Germany*
[23]*Fachbereich Physik, Bergische Universität Wuppertal, Wuppertal, Germany*
[24]*Panjab University, Chandigarh, India*
[25]*Delhi University, Delhi, India*
[26]*Tata Institute of Fundamental Research, Mumbai, India*
[27]*University College Dublin, Dublin, Ireland*
[28]*Korea Detector Laboratory, Korea University, Seoul, Korea*
[29]*CINVESTAV, Mexico City, Mexico*
[30]*Nikhef, Science Park, Amsterdam, the Netherlands*
[31]*Radboud University Nijmegen, Nijmegen, the Netherlands*
[32]*Joint Institute for Nuclear Research, Dubna, Russia*
[33]*Institute for Theoretical and Experimental Physics, Moscow, Russia*
[34]*Moscow State University, Moscow, Russia*
[35]*Institute for High Energy Physics, Protvino, Russia*
[36]*Petersburg Nuclear Physics Institute, St. Petersburg, Russia*
[37]*Institució Catalana de Recerca i Estudis Avançats (ICREA) and Institut de Física d'Altes Energies (IFAE), Barcelona, Spain*
[38]*Uppsala University, Uppsala, Sweden*
[39]*Lancaster University, Lancaster LA1 4YB, United Kingdom*
[40]*Imperial College London, London SW7 2AZ, United Kingdom*
[41]*The University of Manchester, Manchester M13 9PL, United Kingdom*
[42]*University of Arizona, Tucson, Arizona 85721, USA*
[43]*University of California Riverside, Riverside, California 92521, USA*
[44]*Florida State University, Tallahassee, Florida 32306, USA*
[45]*Fermi National Accelerator Laboratory, Batavia, Illinois 60510, USA*
[46]*University of Illinois at Chicago, Chicago, Illinois 60607, USA*
[47]*Northern Illinois University, DeKalb, Illinois 60115, USA*
[48]*Northwestern University, Evanston, Illinois 60208, USA*
[49]*Indiana University, Bloomington, Indiana 47405, USA*

[50]Purdue University Calumet, Hammond, Indiana 46323, USA
[51]University of Notre Dame, Notre Dame, Indiana 46556, USA
[52]Iowa State University, Ames, Iowa 50011, USA
[53]University of Kansas, Lawrence, Kansas 66045, USA
[54]Kansas State University, Manhattan, Kansas 66506, USA
[55]Louisiana Tech University, Ruston, Louisiana 71272, USA
[56]Boston University, Boston, Massachusetts 02215, USA
[57]Northeastern University, Boston, Massachusetts 02115, USA
[58]University of Michigan, Ann Arbor, Michigan 48109, USA
[59]Michigan State University, East Lansing, Michigan 48824, USA
[60]University of Mississippi, University, Mississippi 38677, USA
[61]University of Nebraska, Lincoln, Nebraska 68588, USA
[62]Rutgers University, Piscataway, New Jersey 08855, USA
[63]Princeton University, Princeton, New Jersey 08544, USA
[64]State University of New York, Buffalo, New York 14260, USA
[65]University of Rochester, Rochester, New York 14627, USA
[66]State University of New York, Stony Brook, New York 11794, USA
[67]Brookhaven National Laboratory, Upton, New York 11973, USA
[68]Langston University, Langston, Oklahoma 73050, USA
[69]University of Oklahoma, Norman, Oklahoma 73019, USA
[70]Oklahoma State University, Stillwater, Oklahoma 74078, USA
[71]Brown University, Providence, Rhode Island 02912, USA
[72]University of Texas, Arlington, Texas 76019, USA
[73]Southern Methodist University, Dallas, Texas 75275, USA
[74]Rice University, Houston, Texas 77005, USA
[75]University of Virginia, Charlottesville, Virginia 22901, USA
[76]University of Washington, Seattle, Washington 98195, USA

(Dated: July 2, 2012)

We present measurements of lepton (ℓ) angular distributions in $t\bar{t} \to W^+bW^-\bar{b} \to \ell^+\nu b\ell^-\bar{\nu}\bar{b}$ decays produced in $p\bar{p}$ collisions at a center-of-mass energy of $\sqrt{s} = 1.96$ TeV, where ℓ is an electron or muon. Using data corresponding to an integrated luminosity of 5.4 fb^{-1}, collected with the D0 detector at the Fermilab Tevatron Collider, we find that the angular distributions of ℓ^- relative to anti-protons and ℓ^+ relative to protons are in agreement with each other. Combining the two distributions and correcting for detector acceptance we obtain the forward-backward asymmetry $A_{\rm FB}^{\ell} = (5.8 \pm 5.1(\text{stat}) \pm 1.3(\text{syst}))\%$, compared to the standard model prediction of $A_{\rm FB}^{\ell}(\text{predicted}) = (4.7 \pm 0.1)\%$. This result is further combined with the measurement based on the analysis of the ℓ+jets final state to obtain $A_{\rm FB}^{\ell} = (11.8 \pm 3.2)\%$. Furthermore, we present a first study of the top-quark polarization.

PACS numbers: 14.65.Ha, 12.38.Qk, 13.85.Qk, 11.30.Er

To check the validity of the standard model (SM) of elementary particle physics and to search for possible extensions, we measure the properties of the top (t) quark. At leading order (LO) in perturbative quantum chromodynamics (QCD), production of $t\bar{t}$ pairs through quark-antiquark ($q\bar{q}$) annihilation is expected to be forward-backward (FB) symmetric in the center-of-mass frame. At next-to-leading order (NLO) QCD, interference leads to a positive FB asymmetry, which implies that the top (antitop) quark is emitted with higher probability in the direction of the incoming quark (antiquark). Top pair production through gluon-gluon fusion does not lead to such asymmetry.

SM predictions for the FB asymmetry can be modified by processes beyond the SM [1, 2], such as contributions from hypothesized axigluons [3], Z' or W' bosons [4], and new scalars [5]. These sources of physics beyond the SM modify observables sensitive to the top quark polarization [6].

At the Tevatron $p\bar{p}$ collider, with $\sqrt{s} = 1.96$ TeV, $t\bar{t}$ production is dominated by $q\bar{q}$ annihilation. The direction of the incoming quark (antiquark) therefore coincides with the direction of the proton (antiproton). The t quark (antiquark) is more likely to be emitted in the direction of the incoming quark (antiquark) than in the opposite direction. This FB asymmetry in $t\bar{t}$ production can also be observed through the t and $\bar{t}$ decay products, for example, in the distributions of charged leptons ($\ell = e, \mu$) from $t \to W^+b \to \ell^+\nu b$ and $\bar{t} \to W^-\bar{b} \to \ell^-\bar{\nu}\bar{b}$

*with visitors from [a]Augustana College, Sioux Falls, SD, USA, [b]The University of Liverpool, Liverpool, UK, [c]UPIITA-IPN, Mexico City, Mexico, [d]DESY, Hamburg, Germany, ,[e]SLAC, Menlo Park, CA, USA, [f]University College London, London, UK, [g]Centro de Investigacion en Computacion - IPN, Mexico City, Mexico, [h]ECFM, Universidad Autonoma de Sinaloa, Culiacán, Mexico and [i]Universidade Estadual Paulista, São Paulo, Brazil.

decays.

The CDF and D0 Collaborations have previously performed measurements of the FB asymmetry in $t\bar{t}$ decays to $\ell+$jets final states containing exactly one lepton, jets and an imbalance in transverse momentum ($\not\!\!E_T$) [7–9]. The asymmetries reported by both Tevatron collaborations are larger than predicted in NLO QCD. The asymmetry in CDF data at large values of $t\bar{t}$ invariant mass ($m_t > 450$ GeV) differs by more than three standard deviations (SD) from the NLO prediction [7]. The D0 data show no significant excess in this mass range. Defining a $t\bar{t}$ asymmetry based on the pseudorapidity, η [10], of the charged lepton, D0 finds a significant deviation from NLO QCD predictions of the order of three SD [8]. The ATLAS and CMS collaborations have performed measurements of the difference in angular distributions between top quarks and antiquarks in the $\ell+$jets final state using asymmetries based on the top quark and antiquark rapidities [11, 12] and pseudorapidities [12]. The results are consistent with the SM expectations.

In this Letter, we present six measurements of leptonic FB asymmetries in $p\bar{p}$ collisions at $\sqrt{s} = 1.96$ TeV, using data corresponding to an integrated luminosity of 5.4 fb^{-1}, collected with the D0 detector in Run II of the Fermilab Tevatron Collider. We use $t\bar{t}$ candidates in dilepton final states, where the W bosons from t and $\bar{t}$ decays both decay into $e\nu_e$, $\mu\nu_\mu$, or $\tau\nu_\tau$, and the τ lepton decays leptonically ($\tau \to \ell\nu_\ell\nu_\tau$). We calculate asymmetries based on the pseudorapidity and charge of the electrons or muons. These asymmetries are determined from the angles of the charged leptons, which are measured with high resolution. These measurements have the advantage that a full reconstruction of the $t\bar{t}$ event is not required. In addition, we combine this measurement of the FB asymmetry with the D0 measurement performed in $\ell+$jets final states [8]. Furthermore, we present a first study of the longitudinal polarization of the top quark.

A description of the D0 detector can be found in [13]. The selection criteria and object identification of the dilepton ($ee, e\mu, \mu\mu$) decay channels follow those described in Ref. [14]. To enrich the sample in $t\bar{t}$ events, we require two isolated, oppositely charged leptons with transverse momentum $p_T > 15$ GeV and at least two jets with $p_T > 20$ GeV and detector pseudorapidity $|\eta_{\rm det}| < 2.5$ [10]. For the $e\mu$ channel we require that H_T (defined as the scalar sum of the larger of the two lepton-p_T values and the scalar p_T of each of the two most energetic jets) be greater than 110 GeV. For ee and $\mu\mu$ events we compute a likelihood for the significance of $\not\!\!E_T$ [15], based on the probability distribution calculated from the value of $\not\!\!E_T$ and the lepton and jet energy resolutions. We require this likelihood to exceed the value typical for background events. We find that only the $\mu\mu$ channel benefits from an additional restriction on $\not\!\!E_T$ and, to increase signal purity, we therefore require $\not\!\!E_T > 40$ GeV for the $\mu\mu$ final state. We select a $t\bar{t}$ sample with a signal to background ratio of 3.2, 3.7 and 0.9 in the ee, $e\mu$ and $\mu\mu$ final states, respectively.

To simulate $t\bar{t}$ production, the MC@NLO [16] generator is used assuming $m_t = 172.5$ GeV. The production of top quarks is simulated at NLO, while the decay is simulated only at LO. To include full NLO QCD corrections to both production and decay as well as mixed QCD and quantum electrodynamic corrections and mixed QCD and weak corrections to the production amplitudes (denoted by "QCD+EW"), we simultaneously correct the normalized lepton and antilepton rapidity distributions in MC@NLO using the predictions of Ref. [17]. HERWIG [18] is used to simulate fragmentation, hadronization and decays of short-lived particles, and the generated events are processed through a full detector simulation using GEANT [19]. The Monte Carlo (MC) events are overlaid with data from random bunch crossings to model the effect of detector noise and additional $p\bar{p}$ interactions. The same reconstruction programs are then applied to data and MC events. The background in the dilepton channel arises from $Z/\gamma^* \to \ell^+\ell^-$ and diboson events (WW, WZ and ZZ) with associated jets, from instrumental background where a jet is misidentified as a lepton, and from heavy quarks that decay into leptons that pass isolation requirements. A detailed description of these processes and their generation can be found in Ref. [20].

Leptons are reconstructed with excellent resolution on the measurements of their angles and electric charge. In contrast, it is challenging to reconstruct the four-momenta of the t and $\bar{t}$ quarks, since the kinematics is underconstrained because of the two neutrinos in the final state. Rather than reconstructing the t and $\bar{t}$ four-momenta, as in Refs. [7–9], we measure observables correlated to the FB asymmetry, which depend solely on the η and electric charge of the lepton ℓ, as proposed in Ref. [6]. The asymmetry for leptons is defined as:

$$A^\ell = \frac{N_{\ell^+}(\eta > 0) - N_{\ell^-}(\eta > 0)}{N_{\ell^+}(\eta > 0) + N_{\ell^-}(\eta > 0)}, \qquad (1)$$

where $N_{\ell^-}(\eta)$ and $N_{\ell^+}(\eta)$ correspond to the number of leptons and antileptons as a function of η, respectively. If CP invariance holds in $t\bar{t}$ production and decay, then $N_{\ell^+}(\eta) = N_{\ell^-}(-\eta)$, and $A^\ell_{\rm FB}$ defines the FB asymmetry for both leptons:

$$A^{\ell^\pm}_{\rm FB} = \frac{N_{\ell^\pm}(\eta > 0) - N_{\ell^\pm}(\eta < 0)}{N_{\ell^\pm}(\eta > 0) + N_{\ell^\pm}(\eta < 0)}. \qquad (2)$$

The asymmetries $A^{\ell^+}_{\rm FB}$ and $A^{\ell^-}_{\rm FB}$ are statistically independent and opposite. We can therefore combine the asymmetries for ℓ^+ and ℓ^- by multiplying η with the charge Q of each lepton:

$$A^\ell_{\rm FB} = \frac{N_\ell(Q\cdot\eta > 0) - N_\ell(Q\cdot\eta < 0)}{N_\ell(Q\cdot\eta > 0) + N_\ell(Q\cdot\eta < 0)}. \qquad (3)$$

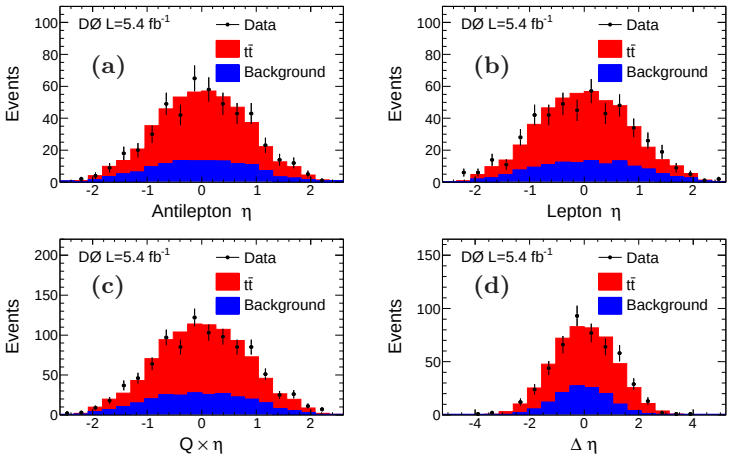

FIG. 1: Pseudorapidity distributions of the charged leptons for the combination of the ee, $e\mu$ and $\mu\mu$ final states after the selection criteria have been applied. The η distribution of positively (a) and negatively (b) charged leptons, the distribution of $Q \cdot \eta$ (c) and the distribution of $\Delta\eta = \eta_{\ell^+} - \eta_{\ell^-}$ (d) are shown. The vertical error bars indicate the statistical uncertainty. The $t\bar{t}$ contribution is normalized to the data after background subtraction.

In analogy to the FB asymmetry for t and $\bar{t}$ quarks, we define an angular asymmetry for leptons:

$$A^{\ell\ell} = \frac{N(\Delta\eta > 0) - N(\Delta\eta < 0)}{N(\Delta\eta > 0) + N(\Delta\eta < 0)}, \quad (4)$$

where $\Delta\eta = \eta_{\ell^+} - \eta_{\ell^-}$. The asymmetry $A^{\ell}_{\rm CP}$ corresponds to a longitudinal asymmetry in spin orientation relative to the proton beam direction. It is defined as:

$$A^{\ell}_{\rm CP} = \frac{N_{\ell^+}(\eta > 0) - N_{\ell^-}(\eta < 0)}{N_{\ell^+}(\eta > 0) + N_{\ell^-}(\eta < 0)}. \quad (5)$$

This asymmetry is sensitive to s-channel exchanges of heavy non-scalar resonances with CP-violating couplings to quarks, but not to possible P and CP-violating effects from an s-channel exchange of Higgs bosons [6].

The asymmetries are measured in four ways using η and Q of the leptons: separate η distributions for (i) ℓ^+ and (ii) ℓ^-, (iii) the charge-signed pseudorapidity, $Q \cdot \eta$, and (iv) $\Delta\eta$. They are presented in Fig. 1. To extract the asymmetries for $t\bar{t}$ events from the distributions shown in Fig. 1, we subtract the background and then correct for effects from event reconstruction and acceptance. The correction for detector acceptance is performed by multiplying the background-subtracted number of events with the inverse of the selection efficiency. This is calculated using $t\bar{t}$ MC events, where we evaluate the selection efficiency separately for twenty bins in lepton η, to reduce the model dependence of our acceptance correction and to provide sufficient MC statistics.

The resolution of the measurement of lepton η is obtained from studies of $t\bar{t}$ MC events by comparing the generated value of η with the value measured following event reconstruction. For electrons and muons, we use the η of tracks measured in the tracking system and find this resolution to be the same for both types of leptons. This resolution is also investigated using cosmic-ray muons that appear as dimuon events and is found to be ≈ 0.0026, consistent with the MC expectation. For $\approx 99.8\%$ of the electrons or muons in $t\bar{t}$ MC events, the sign of lepton η is correctly reconstructed. Migration of events within the "forward" or "backward" regions does not affect the reconstructed angular asymmetry except for negligible acceptance corrections. The reconstruction effects on the measurement of η can therefore be neglected for charged leptons.

The Z+jets background, which is predicted through MC simulation [20], contributes to the asymmetry. To study the influence of the Z+jets background, we perform measurements of all six asymmetries in a sample dominated by Z+jets production in final states with two electrons or two muons. Applying the same event selections as for the final $t\bar{t}$ enriched sample, except for the $\not\!\!E_T$ significance likelihood and $\not\!\!E_T$ requirements, all asymmetries are measured using the same procedure as for the measurement of $t\bar{t}$ asymmetries, but treating Z+jets as "signal" and $t\bar{t}$ as "background". In this control sample, all other background contributions are negligible. The data and MC predictions for the η distribution of positively and negatively charged leptons, for $Q \cdot \eta$, and $\Delta\eta$, are in good agreement, as presented in [21].

To verify that the measurement of the $t\bar{t}$ asymmetries is unbiased and correctly estimates the statistical uncertainty of the result, we perform the measurement using ensembles of MC pseudo-experiments. To obtain samples with different asymmetries, we mix a $t\bar{t}$ MC event sample weighted to have no asymmetry with different fractions of $t\bar{t}$ MC events with a SM asymmetry. We fluctuate the expected number of events in the "forward" and "backward" direction for each pseudo-experiment assuming Poisson statistics and apply the same procedure as for data to extract the asymmetry. This test shows that the measurement is unbiased and that the statistical uncertainties are estimated correctly.

Systematic uncertainties can affect the distributions in lepton η. In particular, the energy scale for jets, jet energy resolution, jet reconstruction, the normalization of background, the MC-derived acceptance, and the finite number of MC events can shift the measured asymmetry. The normalization of the background has uncertainties from diboson and Z+jets cross sections, as well as a 6.1% uncertainty on the data sample's integrated luminosity. The systematic uncertainties on the light and heavy-flavor jet energy scales, jet energy resolution, and the jet reconstruction can affect the acceptance. We evaluate the size of these uncertainties by applying the variation in acceptance corrections and in the differential distribution of lepton η in deriving the $t\bar{t}$ asymmetry.

In addition, we compare the acceptance from single leptons obtained from simulated $t\bar{t}$ events with the accep-

TABLE 1: Systematic uncertainties for the six unfolded asymmetries defined in Eqs. (1)-(5) for the combination of all dilepton final states. All values are given in %.

Source	A^{ℓ}	$A^{\ell^+}_{\rm FB}$	$A^{\ell^-}_{\rm FB}$	$A^{\ell}_{\rm FB}$	$A^{\ell\ell}$	$A^{\ell}_{\rm CP}$
Jets	1.1	0.8	1.7	1.0	1.5	1.2
MC statistics	0.4	0.4	0.4	0.3	0.5	0.3
Bkg normalization	0.3	0.3	0.6	0.3	0.7	0.3
Acceptance	0.7	0.2	1.5	0.7	2.3	0.9
Total	1.4	1.1	2.4	1.3	2.9	1.6

TABLE 2: Measured asymmetries for leptons, as defined in Eqs. (1)-(5), including statistical and systematic uncertainties for the combined dilepton final states using raw and unfolded distributions are compared to predictions from MC@NLO including QCD+EW corrections. Our predictions are calculated using the NLO QCD+EW distributions in both numerator and denominator of Eqs. (1)-(5). This is different to the calculations in Refs. [6, 17] where the denominator is calculated in LO QCD to derive expressions for the asymmetries of $\mathcal{O}(\alpha_s)$. All values are given in %.

	Raw	Unfolded	Predicted
A^{ℓ}	$2.9 \pm 6.1 \pm 0.9$	$2.5 \pm 7.1 \pm 1.4$	4.7 ± 0.1
$A^{\ell^+}_{\rm FB}$	$4.5 \pm 6.1 \pm 1.1$	$4.1 \pm 6.8 \pm 1.1$	4.4 ± 0.2
$A^{\ell^-}_{\rm FB}$	$-1.2 \pm 6.1 \pm 1.3$	$-8.4 \pm 7.4 \pm 2.4$	-5.0 ± 0.2
$A^{\ell}_{\rm FB}$	$3.1 \pm 4.3 \pm 0.8$	$5.8 \pm 5.1 \pm 1.3$	4.7 ± 0.1
$A^{\ell\ell}$	$3.3 \pm 6.0 \pm 1.1$	$5.3 \pm 7.9 \pm 2.9$	6.2 ± 0.2
$A^{\ell}_{\rm CP}$	$1.8 \pm 4.3 \pm 1.0$	$-1.8 \pm 5.1 \pm 1.6$	-0.3 ± 0.1

tance obtained from $Z \to \ell^+\ell^-$ data. We select a data sample enriched in $Z \to \ell^+\ell^-$ events, where one lepton is required to pass tight lepton-selection criteria to function as a "tag" and the other "probe" lepton to pass a loose lepton selection. The acceptance is evaluated as function of η by applying a tight-lepton identification requirement on the probe. No significant difference is observed between the acceptance for positive or negative pseudorapidities, nor between positively and negatively charged leptons. A systematic uncertainty on the acceptance is defined for each lepton charge by the difference in acceptance between the forward and backward hemisphere of the detector. This study is performed separately for electrons and muons. The systematic uncertainties are added in quadrature to yield the total systematic uncertainties given in Table 1.

Using the distributions in Fig. 1, the lepton asymmetries of Eqs. (1)-(5) are measured and corrected for acceptance effects ("unfolded"). The measurements of the uncorrected (raw) asymmetries as well as the unfolded asymmetries are compared to the predictions from MC@NLO including QCD+EW corrections [6] in Table 2. All unfolded asymmetries are in agreement with the SM predictions.

The asymmetry $A^{\ell}_{\rm FB}$ defined in Eq. (2) is also measured in ℓ+jets final states [8]. The result for $A^{\ell}_{\rm FB} = (15.2 \pm 4.0)\%$ is compared to a predicted value from MC@NLO of $(2.1 \pm 0.1)\%$. We checked that the predicted asymmetry is independent of the final state and the difference to our prediction of $(4.7 \pm 0.1)\%$ is only due to the QCD+EW corrections. The dominant systematic uncertainty on the prediction and on our measurement in dilepton final states is given by jet reconstruction related systematics. The total uncertainty of the measurement is dominated by the statistical component. Since the ℓ+jets and dilepton final states are selected to be statistically independent, we can improve the uncertainty on $A^{\ell}_{\rm FB}$ by combining both measurements.

The combination of the two asymmetries $A^{\ell}_{\rm FB}$ is performed using the BLUE method [22, 23]. All systematic uncertainties evaluated in both measurements are treated as fully correlated. The combination yields a leptonic FB asymmetry of $A^{\ell}_{\rm FB} = (11.8 \pm 3.2)\%$, where the ℓ+jets channel contributes 63.9% and the dilepton channel 36.1% of the information. This represents an improvement of about 20% relative to the uncertainty in the ℓ+jets channel alone. The consistency between the two individual measurements is 68%. Comparing the combined result to the predicted leptonic FB asymmetry from MC@NLO plus higher order QCD+EW corrections, $A^{\ell}_{\rm FB}$(predicted) $= (4.7 \pm 0.1)\%$, we observe a disagreement at the level of 2.2 SD.

To further investigate this deviation of the asymmetry from the SM prediction, we analyze the longitudinal polarization of the top quark. While in the SM top quarks are expected to be produced unpolarized in $t\bar{t}$ events, there are many beyond the SM models that would enhance the $t\bar{t}$ FB asymmetry [1] and therefore the leptonic asymmetries defined in Eqs. (1)-(5), and would also lead to a non-vanishing longitudinal polarization of the top quark. Examples are models with new parity-violating interactions. In the absence of effects from acceptance, the distribution of $\cos\theta^-$ and $\cos\theta^+$ should be isotropic [6] for unpolarized top quarks, where θ^+ (θ^-) is the angle between the direction of the ℓ^+ (ℓ^-) in the t ($\bar{t}$) rest frame and the t ($\bar{t}$) direction in the $t\bar{t}$ rest frame. A longitudinal polarization of the top quark would cause asymmetric $\cos\theta^{\pm}$ distributions.

Assuming CP invariance, i.e. that the distributions of $\cos\theta^+$ and $\cos\theta^-$ are equal, we measure the distribution $\cos\theta$, defined by the sum of the $\cos\theta^{\pm}$ distributions. The calculation of the angles $\theta^{\pm}$ requires a transformation of the momenta of the charged leptons into the t and $\bar{t}$ quark rest frames. Every event must therefore be fully reconstructed. This is performed using the neutrino weighting method, devised originally to measure the top quark mass in the dilepton channel [24] and recently applied to measure $t\bar{t}$ spin correlations [20].

In Fig. 2, the $\cos\theta$ distribution is shown separately for the dilepton and ℓ+jets final states. The distribution for $t\bar{t}$ events produced via a leptophobic topcolor Z' boson, with the same parity-violating couplings to quarks as the SM Z boson and a width $\Gamma = 0.012 M_{\rm Z}$ [25, 26] is also

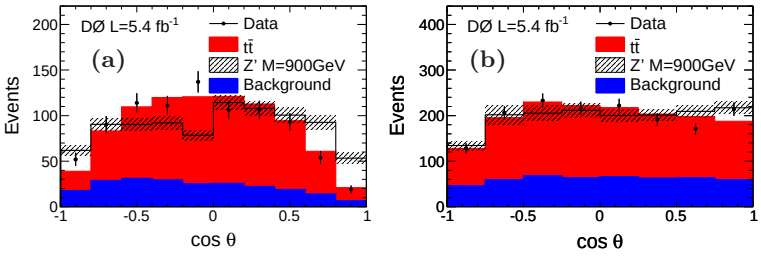

FIG. 2: The distribution of $\cos\theta$ is shown for the combination of the dilepton channels (a) and the ℓ+jets channels (b). The data are compared to the SM predictions. The vertical errorbars on the data points indicate the statistical uncertainty of the data. The distribution of $t\bar{t}$ pairs produced via a hypothetical Z' boson is also shown; the uncertainty due to the limited size of the MC sample is shown by the shaded band. The same Z' model as in [25, 26] is used.

shown to illustrate the effect of producing t and $\bar{t}$ quarks with longitudinal polarization. The agreement between the data and the SM prediction in both distributions is good, yielding a Kolmogorov-Smirnov test probability of 14% in the dilepton channel and 58% in the ℓ+jets channel. There is no significant hint of new sources of parity violation leading to a longitudinal polarization in $t\bar{t}$ production.

In conclusion, we measured angular asymmetries in $t\bar{t}$ production based on η distributions of charged leptons. We find the leptonic FB asymmetry $A^{\ell}_{\rm FB}$ and the lepton asymmetry $A^{\ell\ell}$ in agreement with the SM prediction in the dilepton final state. Combining our measurement of $A^{\ell}_{\rm FB}$ with the measurement performed using leptons in ℓ+jets final states yields $A^{\ell}_{\rm FB} = (11.8 \pm 3.2)\%$, which is 2.2 SD above the higher order QCD+EW prediction of $A^{\ell}_{\rm FB}({\rm predicted}) = (4.7 \pm 0.1)\%$. The top-quark polarization in the dilepton and ℓ+jets final states show good agreement between the data and the SM prediction.

Acknowledgments

We would like to thank W. Bernreuther and Z. G. Si for useful discussions and providing us with the lepton rapidity distributions used for theoretical predictions. We thank the staffs at Fermilab and collaborating institutions, and acknowledge support from the DOE and NSF (USA); CEA and CNRS/IN2P3 (France); FASI, Rosatom and RFBR (Russia); CNPq, FAPERJ, FAPESP and FUNDUNESP (Brazil); DAE and DST (India); Colciencias (Colombia); CONACyT (Mexico); NRF (Korea); CONICET and UBACyT (Argentina); FOM (The Netherlands); STFC and the Royal Society (United Kingdom); MSMT and GACR (Czech Republic); BMBF and DFG (Germany); SFI (Ireland); The Swedish Research Council (Sweden); and CAS and CNSF (China).

[1] D. Krohn, T. Liu, J. Shelton, and L.-T. Wang, Phys. Rev. D **84**, 074034 (2011).
[2] J. A. Aguilar-Saavedra, arXiv:1202.2382 [hep-ph].
[3] A. Djouadi, G. Moreau, F. Richard, and R. K. Singh, Phys. Rev. D **82**, 071702 (2010); R. Barcelo, A. Carmona, M. Masip, and J. Santiago, Phys. Lett. B **707**, 88 (2012); G. M. Tavares and M. Schmaltz, Phys. Rev. D **84**, 054008 (2011); E. Alvarez, L. Da Rold, J. I. S. Vietto, and A. Szynkman, J. High Energy Phys. **09**, 007 (2011); J. A. Aguilar-Saavedra and M. Perez-Victoria, Phys. Lett. B **705**, 228 (2011).
[4] S. Jung, H. Murayama, A. Pierce, and J. D. Wells, Phys. Rev. D **81**, 015004 (2010); K. Cheung, W.-Y. Keung, and T.-C. Yuan, Phys. Lett. B **682**, 287 (2009).
[5] J. A. Aguilar-Saavedra and M. Perez-Victoria, J. High Energy Phys. **09**, 097 (2011).
[6] W. Bernreuther and Z. -G. Si, Nucl. Phys. B **837**, 90 (2010).
[7] T. Aaltonen *et al.* [CDF Collaboration], Phys. Rev. D **83**, 112003 (2011).
[8] V. M. Abazov *et al.* [D0 Collaboration], Phys. Rev. D **84**, 112005 (2011).
[9] V. M. Abazov *et al.* [D0 Collaboration], Phys. Rev. Lett. **100**, 142002 (2008).
[10] The rapidity y and pseudorapidity η of a particle are defined as functions of the polar angle θ with respect to the proton beam direction and velocity β as $y(\theta,\beta) \equiv \frac{1}{2}\ln[(1+\beta\cos\theta)/(1-\beta\cos\theta)]$ and $\eta(\theta) \equiv y(\theta,1)$, where β is the ratio of a particle's momentum to its energy. We distinguish detector η ($\eta_{\rm det}$) and collision η, where the former is defined with respect to the center of the detector and the latter with respect to the $p\bar{p}$ interaction vertex.
[11] G. Aad *et al.* [ATLAS Collaboration], arXiv:1203.4211 [hep-ex].
[12] S. Chatrchyan *et al.* [CMS Collaboration], Phys. Lett. B **709**, 28 (2012).
[13] V. M. Abazov *et al.* [D0 Collaboration], Nucl. Instrum. Methods Phys. Res. A **565**, 463 (2006); M. Abolins *et al.*, Nucl. Instrum. Methods Phys. Res. A **584**, 75 (2008); R. Angstadt *et al.*, Nucl. Instrum. Methods Phys. Res. A **622**, 298 (2010).
[14] V. M. Abazov *et al.* [D0 Collaboration], Phys. Lett. B **704**, 403 (2011).
[15] A. G. Schwartzman, Fermilab-Thesis-2004-21 (2004).
[16] S. Frixione and B. R. Webber, J. High Energy Phys. **06**, 029 (2002).
[17] W. Bernreuther and Z. -G. Si, arXiv:1205.6580 [hep-ph].
[18] G. Corcella *et al.*, J. High Energy Phys. **01**, 010 (2001).
[19] R. Brun and F. Carminati, CERN Program Library Long Writeup W5013, 1993 (unpublished).
[20] V. M. Abazov *et al.* [D0 Collaboration], Phys. Lett. B **702**, 16 (2011).
[21] See Appendix A for additional figures of the η distribution of positively and negatively charged leptons, for $Q\cdot\eta$, and $\Delta\eta$, in a sample dominated by Z+jets background.
[22] L. Lyons, D. Gibaut, and P. Clifford, Nucl. Instrum.

Appendix A

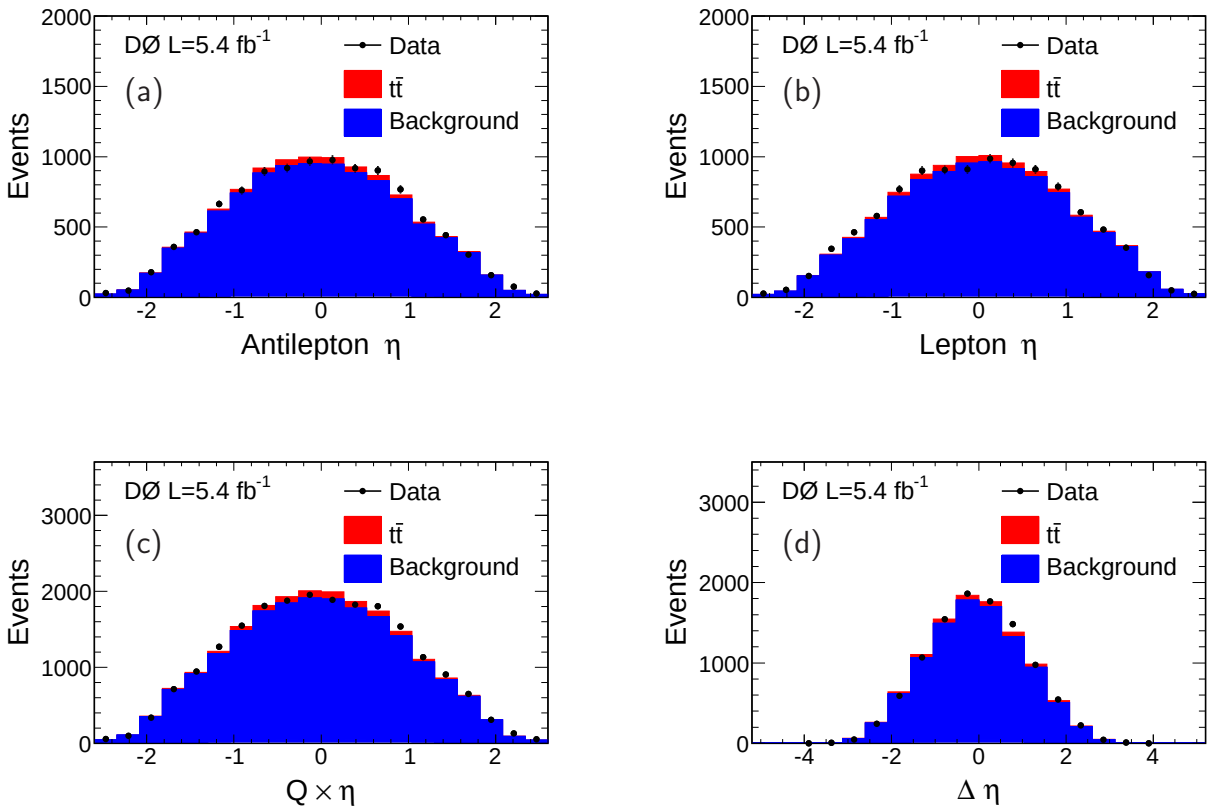

FIG. 3: Rapidity distributions of the charged leptons for the combination of the dimuon and dielectron final states. The final selection requirements have been removed i.e. the $\not\!\!E_T$ significance likelihood cut for the ee and $\mu\mu$ channels and the $\not\!\!E_T$ cut for the $\mu\mu$ final state. The samples are therefore dominated by Z+jets events. The pseudorapidity distribution of positively (a) and negatively (b) charged leptons, the distribution of $q \cdot \eta$ (c) and the distribution of $\Delta\eta = \eta_{\ell^+} - \eta_{\ell^-}$ (d) are shown.

Methods in Phys. Res. Sect. A **270**, 110 (1988).
[23] A. Valassi, Nucl. Instrum. Methods in Phys. Res. Sect. A **500**, 391 (2003).
[24] V. M. Abazov *et al.* [D0 Collaboration], Phys. Rev. D **80**, 092006 (2009); B. Abbott *et al.* [D0 Collaboration], Phys. Rev. Lett. **80**, 2063 (1998).
[25] R. M. Harris, C. T. Hill, and S. J. Parke, hep-ph/9911288.
[26] V. M. Abazov *et al.* [D0 Collaboration], Phys. Rev. D **85**, 051101 (2012).